Prune cAMP phosphodiesterase binds nm23-H1 and promotes cancer metastasis

Anna D'Angelo,[1] Livia Garzia,[1] Alessandra André,[1] Pietro Carotenuto,[1] Veruska Aglio,[1] Ombretta Guardiola,[1] Gianluigi Arrigoni,[2] Antonio Cossu,[3] Giuseppe Palmieri,[4] L. Aravind,[5] and Massimo Zollo[1,*]

[1]Telethon Institute of Genetics and Medicine, Via Pietro Castellino 111, 80131 Naples, Italy
[2] Department of Anatomy and Pathology, Ospedale San Raffaele, HSR, Milan, Italy
[3] Azienda A.S.L. n° 1, Sassari, Department of Pathology, University of Sassari, Italy
[4] Istituto di Chimica Biomolecolare, Sezione di Sassari, Consiglio Nazionale delle Ricerche Tramariglio, Alghero, Italy
[5] Computational Biology Branch, National Institutes of Health, National Center for Biotechnology Information, The National Library of Medicine, Bethesda, Maryland 20894
*Correspondence: zollo@tigem.it

Summary

We identify a new enzymatic activity underlying metastasis in breast cancer and describe its susceptibility to therapeutic inhibition. We show that human prune (h-prune), a phosphoesterase DHH family appertaining protein, has a hitherto unrecognized cyclic nucleotide phosphodiesterase activity effectively suppressed by dipyridamole, a phosphodiesterase inhibitor. H-prune physically interacts with nm23-H1, a metastasis suppressor gene. The h-prune PDE activity, suppressed by dipyridamole and enhanced by the interaction with nm23-H1, stimulates cellular motility and metastasis processes. Out of 59 metastatic breast cancer cases analyzed, 22 (37%) were found to overexpress h-prune, evidence that this novel enzymatic activity is involved in promoting cancer metastasis.

Introduction

The human prune (h-prune) protein belongs to the DHH superfamily, which includes several phosphoesterases, such as the RecJ nuclease from bacteria and the pyrophosphatases from yeast and bacteria (Aravind and Koonin, 1998b). The DHH superfamily can be divided into two main groups on the basis of a C-terminal motif that is very well conserved within each group but not across the groups. All of the members of this superfamily possess four other motifs that contain highly conserved charged residues that are predicted to be responsible for binding ions and catalyzing the phosphoesterase reaction. The most characteristic of these is the third motif, with the signature DHH (Asp-His-His), after which this superfamily was named. The RecJ protein is a DNA repair protein and, along with other nucleases and poorly characterized bacterial proteins, belongs to the first group. Prune and the polyphosphatases belong to the second group. The recent availability of the structures of the RecJ protein (Yamagata et al., 2002) and the bacterial pyrophosphatases (PPASEs) (Ahn et al., 2001) reveal that these two major classes of DHH proteins share an N-terminal α/β domain with a five-stranded parallel sheet but have somewhat different C-terminal domains. The first four motifs are the most conserved portions of the N-terminal domain and define the active site of these enzymes, whereas the group-specific fifth motif maps to the divergent C-terminal domains.

The *Drosophila prune* gene was originally characterized based on its mutant phenotype, which showed a brownish-purple eye color due to the reduction of drosopterins, in contrast to the bright red eye of the wild-type fly (Timmons and Shearn, 1996). While homozygous *prune* mutants are viable and fertile, they are synthetically lethal, developing pseudomelanotic tumors in the presence of even a single copy of the gain-of-function mutation in the abnormal wing disc gene (*awd/K-pn*; also named Killer-of-Prune). Humans encode up to eight orthologs of *awd* (nm23s), at least four of which are active nucleoside diphosphate kinases (NDPKs), which catalyze the phosphoryl transfer from a nucleoside triphosphate to a nucleoside diphosphate (Lombardi et al., 2000). One of these, nm23-H1 (NDPK-A), is a predominantly cytoplasmic protein with antimetastatic properties, and mutations in it are associated with the progression of cancers. Numerous tumors and highly proliferative cells overexpress nm23-H1 mRNA and protein, and in most cases this overexpression is linked to early stages of cancer,

SIGNIFICANCE

H-prune is frequently overexpressed, and nm-23 is often downregulated in metastatic cancers in different tissues. Our work provides mechanistic insight into how the interaction between these molecules can control cancer metastasis. A major pathway identified by this work is the binding of nm23-H1 and h-prune with physiological consequences. By identifying a novel enzymatic activity of h-prune required for its metastasis-promoting potential, these results open the possibility of therapeutic intervention. Dipyridamole, a selective inhibitor of h-prune activity, is already used in the clinic, which could facilitate clinical trials to address its potential use as a suppressor of metastasis.

with a loss of expression in more advanced and aggressive stages. In breast cancer and in melanomas, high expression of human nm23-H1 is associated with a decreased metastatic potential (Florenes et al., 1992). In contrast, in other cancers, such as prostate, non-Hodgkin lymphomas, and neuroblastomas, high nm23-H1 expression is associated with an adverse outcome (Hartsough and Steeg, 2000; Niitsu et al., 2001). To date, several mutations that affect nm23s folding, oligomerization, DNA binding, or NDPK activity have been described for nm23-H1. In particular, the nm23H1-P96S mutation, a *Drosophila* developmental mutation homolog (*awd/K-pn*), exhibits autophosphorylation and NDPK normal function, while it is deficient for phosphotransferase activity and shows failure in folding properties associated to oligomeric nm23-H1 protein complexes (Freije et al., 1997a). A second mutation, nm23H1-S120G, associated with stage IV-S neuroblastoma (Chang et al., 1994) shows a positive effect on tumor cell motility (MacDonald et al., 1996).

In breast cancer, metastatic spread is responsible for virtually all cancer deaths. Metastasis is a highly complex molecular and cellular process (Sleeman, 2000). To become invasive, tumor cells need to change their adhesive properties in order to lose contact with other cells in the primary tumor and make new contacts with the extracellular matrix of host cells that they encounter as they invade. They also need to be able to penetrate into the surrounding host tissue, and here the modulation of protease activity in the vicinity of the tumor cells plays a critical role. To migrate away from the primary tumor, tumor cells also need to gain motility functions. These same properties are also thought to be important when circulating tumor cells exit the circulatory system and start metastatic colonization in secondary organs. To date, several metastasis suppressor genes have been isolated and characterized (Steeg, 2003). Within this group, nm23 plays a major role for its ability to induce low motility cellular processes if overexpressed in aggressive breast cancer cells (Freije et al., 1997a, 1997b; Hartsough et al., 2001), influencing anchorage-independent colonization and induction to differentiation (Kantor et al., 1993; Leone et al., 1993a; Howlett et al., 1994; Hartsough and Steeg, 1998; Lombardi et al., 2000). Of note is a new role of nm23-H1, alternatively named GzmA-activated Dnase, which creates single-stranded DNA nicks in the nucleus in a caspase-independent apoptosis pathway (Fan et al., 2003).

Our group has previously demonstrated the interaction between h-prune and nm23-H1 and the disruption of this interaction by the nm23H1-S120G mutation (Reymond et al., 1999). In addition, we have demonstrated that amplification of *h-prune* copy numbers induces cell proliferation and that high levels of h-prune expression, compared to the moderate or low nm23-H1 levels, is correlated to aggressiveness of sarcoma and breast carcinoma tumors, thus postulating an inhibitory role of h-prune versus the suppressor of metastasis nm23 function in vivo (Forus et al., 2001). Given the h-prune prediction of a phosphoesterase activity and its association with NDPK family proteins, we have investigated its precise biochemical properties and its potential role in metastasis. We demonstrate that h-prune has phosphodiesterase (PDE) activity, with a preferential affinity for cAMP over cGMP as substrate. PDEs belong to a diverse superfamily that catalyze the hydrolysis of 3′,5′-cyclic nucleotides (cAMP; cGMP) to their corresponding nucleoside 5′-monophosphates (Beavo and Brunton, 2002). In addition, as overexpression of nm23-H1 in the aggressive breast cancer cell line clone MDA-C100 has been shown to significantly reduce its metastatic phenotype both in vitro and in vivo (Hartsough and Steeg, 2000; Mao et al., 2001; Tseng et al., 2001), we show that h-prune is able to change the "low" motility phase to a "high" motility phase. In a panel of eight PDE selective inhibitors tested, dipyridamole, an anti-platelet aggregation drug, was found to inhibit h-prune PDE activity both in vitro and in our cellular breast model. Further in vivo analyses in a large number of metastatic breast tumors showed a direct correlation between h-prune protein increased levels and lower regulation of nm23-H1 expression, thus leading to the formation of distal metastasis as reported in our clinical follow-up records. A direct correlation between an increased h-prune cAMP-PDE activity and cellular motility, due to a physical protein-protein interaction with nm23-H1, was found in the breast cancer model.

These findings throw light on the interaction between h-prune and nm23-H1, altering its protective function in cellular proliferation and tumor metastasis processes. Thus, this represents a novel cellular pathway that is involved in terminal differentiation and malignancy of tumors.

Results

Structural and functional analysis of h-prune

An iterative protein database search (PSI-BLAST) initiated on the h-prune protein recovered, with statistically significant expectation values, the eukaryotic orthologs of prune, followed by the inorganic pyrophosphatases from a variety of bacteria and diverse DHH proteins from various organisms, including the RecJ nucleases (Figures 1A and 1C). A clustering of the DHH proteins using the BLASTCLUST program and a phylogenetic analysis using the maximum likelihood method show that prune proteins (human and *Drosophila*) belong to the second DHH family, along with the inorganic pyrophosphatases (Figure 1A). While the two families of DHH proteins share a common N-terminal domain that contains the four conserved motifs typical of the DHH superfamily, they are distinguished from each other by their C-terminal domains. The shared N-terminal domain has an α/β fold with a parallel β sheet and contains the motifs with the absolutely conserved signatures of the form DXD (Motif-I), D (Motif-II), DHH (Motif-III), and D/E (Motif-IV) (Figures 1A and 1B). These residues are all on the same face of this domain and together form the catalytic site that chelates at least two divalent cations. The prune proteins contain the form DHR as substitution for the canonical DHH (Motif-III) that is observed in all other members of this family (Figure 1A). In both DHH families, the C-terminal domain contains a core sheet of five strands, four of which form two β strand hairpins. However, differences in the C-terminal domains between the first and the second families of DHH proteins may contribute prominently to substrate specificities of the two superfamilies. Additionally, C-terminal to the DHH module, mammalian prune contains a nonglobular extension, within which there are some conserved serines that may serve as a site for regulation through phosphorylation.

Structural analysis of h-prune showed similarities to RecJ (Yamagata et al., 2002) and pyrophosphatases proteins (Ahn et al., 2001), thus suggesting potentially similar activities to those proteins. However, their strong synergistic interactions with the awd/K-pn-like NDPKs suggested that prune proteins might have alternative substrates, such as nucleotides. Evolutionary studies

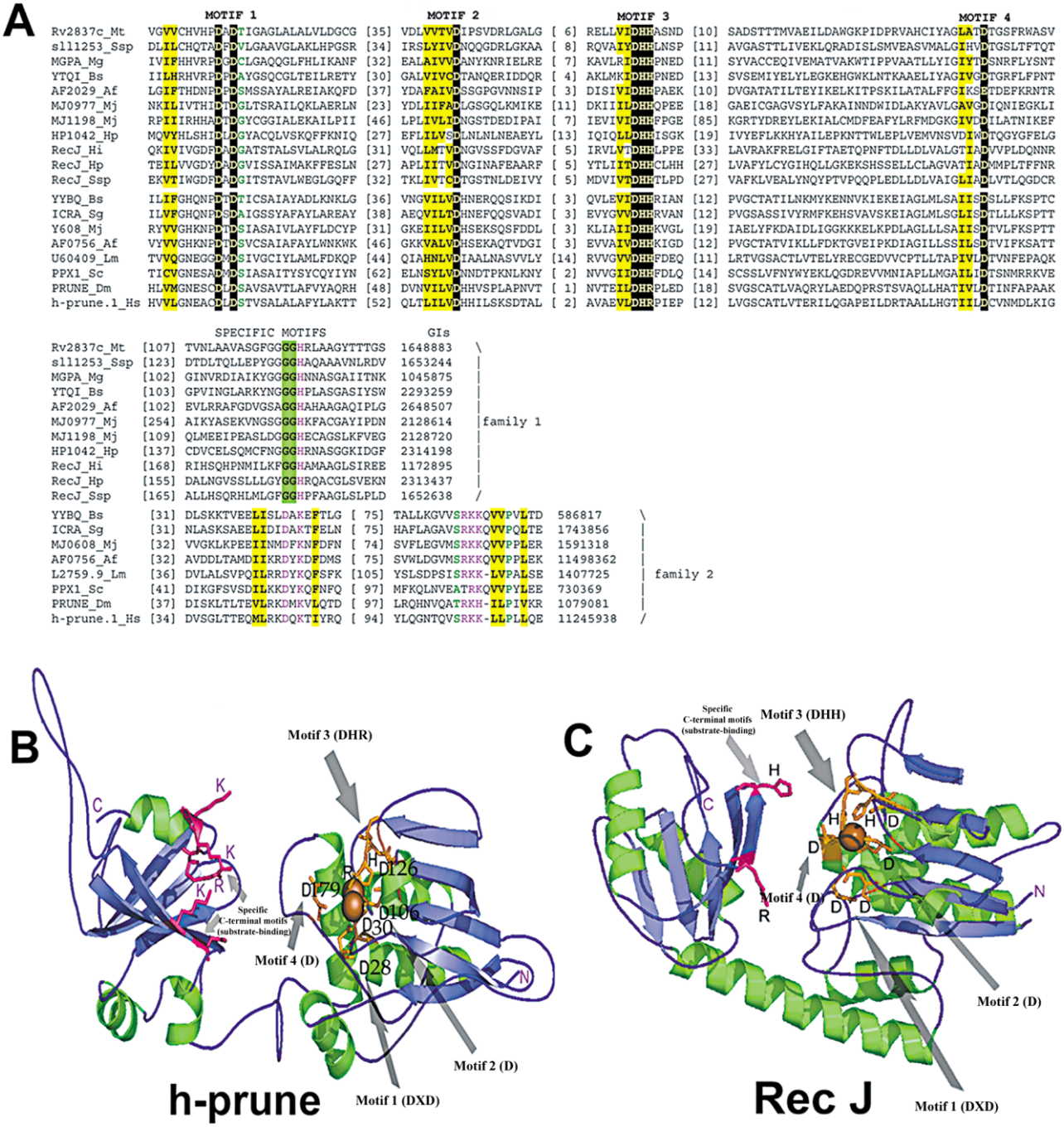

Figure 1. Alignment of DHH family phosphoesterases

A: Multiple alignment of the DHH family phosphoesterases, showing separately the four generic motifs (I–IV) and the motifs diagnostic of the two distinct subfamilies that map to the second domain. The position of the first aligned residue in each protein sequence and the distances between the motifs are indicated by numbers. The Gene Identification (GI) numbers in the NCBI/GenBank protein sequence database are indicated to the right of each sequence. Species name abbreviations: Af, *Archaeoglobus fulgidus*; Bb, *Borrelia burgdorferi*; Bs, *Bacillus subtilis*; Dm, *Drosophila melanogaster*; Ec, *Escherichia coli*; Hi, *Hameophilus influenzae*; Hp, *Helicobacter pylori*; Lm, *Leishmania major*; Mg, *Mycoplasma genitalium*; Mj, *Methanococcus jannaschii*; Mp, *Mycoplasma pneumoniae*; Mt, *Mycobacterium tuberculosis*; Sc, *Saccharomyces cerevisiae*; Sg, *Streptococcus gordonii*; Ssp, *Synechocystis species*.

B: Ribbon structure of the h-prune protein based on the crystal structure of PPASE and the RecJ protein. Red balls indicate potential cofactor ions (Mg^{2+} and/or Mn^{2+}) and the region of binding to motif III. Arrows indicate the aspartic acids (D). Aspartic acids of the four DHH motifs are represented, indicating the potential catalytic site of DHH protein family.

C: Ribbon structure of the RecJ protein. Red balls indicate cofactor ions (Mg^{2+} and/or Mn^{2+}) and the region of binding to motif III. Arrows indicate the aspartic acids (D) characteristic of DHH protein family.

on the DHH family have shown that phosphoesterases are derived from a number of protein folds that encode diverse phosphoesterases and hydrolases. These include the HD fold, from which the classic signaling PDEs are recognized (PDE1-11) (Aravind and Koonin, 1998a, 1998b; Galperin et al., 1999); the metallo-β-lactamase fold (Galperin et al., 1999; Aravind, 1999), from which the PdsA-like PDEs have derived; and the calcineurin-like phosphoesterase fold (Aravind and Koonin, 1998b), from which Icc-like PDEs have derived. While the DHH catalytic domain has a very distinct fold from these other families, it contains several analogous metal chelating residues (aspartates and histidines) and could potentially define an entirely new class of PDEs. In order to test this hypothesis, we expressed, purified, and assayed h-prune for potential PDE activity.

Identification and characterization of the h-prune phosphodiesterase activity

To determine the ability of h-prune to disrupt the phosphoester bonds in cyclic nucleotides (cAMP and cGMP), we cloned and expressed h-prune using the Baculovirus expression system. His-tagged h-prune and h-pruneΔ, a mutation created in the motif III region (DHRP126-129AAAA), were purified by affinity chromatography. We used the PDE assay to characterize purified h-prune catalytic activity and to determine the specific substrate. As shown in Figure 2A, h-prune possesses significant PDE activity that is higher for cAMP than for cGMP as substrate, while h-pruneΔ shows a 40% reduction of this activity. As positive control, we used PDE2. The negative controls were both h-prune preincubated with the A59-specific polyclonal antibody and h-pruneΔ (Figure 2A). To confirm the PDE activity found, we overexpressed h-prune and h-pruneΔ transiently in human HEK-293 cells, followed by immunoprecipitation and then performed a PDE assay on immunoprecipitated proteins (data not shown). These results indicate that h-prune protein, purified both from insect and human cells, shows PDE activity.

To identify amino acids potentially involved in the catalytic site, a mutation analysis at single and multiple sites affecting h-prune PDE activity was conducted. All the aspartic acids of the DHH characteristic motifs (Figure 1B) were mutated alone and in combination (Figure 2B). We expressed the mutants using the Baculovirus expression system and purified them to homogeneity (with an 80% yield of purification). We tested the proteins for cAMP-PDE activity and observed an 80% decrease in the h-prune4DΔ (D28A, D106A, Δ, D179A) mutant. In summary, D28, D126, H127, R128, P129, and D179 amino acids were found to be essential for h-prune PDE activity, thus indicating that they are most likely part of the catalytic site. Instead, D106A mutation in motif II did not influence h-prune PDE activity.

To define K_m values, we purified the His-tagged h-prune protein to homogeneity by another step of purification using an ion-exchange chromatography (Mono-Q column) with a high yield of purification (90%). The K_m and V_{max} values were determined by measuring nucleotides hydrolysis with a fixed amount of purified enzyme in a range of substrate concentrations (0.05–10.0 μM) and taking those data points in the linear part of the reaction. Both cAMP and cGMP are substrates for h-prune, with K_m values of 0.9 ± 0.03 μM and 2.3 ± 0.11 μM, respectively (Figures 2C and 2D). The maximal rates of turnover of substrate (V_{max}) were found to be 12.8 ± 0.5 pmol $\times$ min^{-1} $\times$ μg^{-1} and 16.1 ± 0.8 pmol $\times$ min^{-1} $\times$ μg^{-1} purified enzyme for cAMP and cGMP, respectively. These data were also verified by an alternative phosphodiesterase assay (Fisher et al., 1998) (data not shown). Thus, we present evidence of a cyclic nucleotide phosphodiesterase activity for a protein of the DHH superfamily. To study the buffer influence on h-prune PDE activity, we tested Tris-HCl and HEPES buffers in the presence of the same salt, and we observed a higher PDE activity in the presence of Tris-HCl buffer (Figure 2E). Considering the ion dependence of DHH proteins, we investigated the Mg^{2+} and Mn^{2+} ion dependency of h-prune in the PDE cAMP assay. Although the higher activity of h-prune was found in Tris-HCl buffer, we performed PDE assays, using increasing concentrations of two different divalent ions, in the presence of HEPES buffer to avoid oxido-reduction reactions. Although some PDE activity was measured in the no-ion buffer, Mg^{2+} stimulated h-prune PDE activity (Figure 2E). In contrast, in the presence of $MnCl_2$, this activity is inhibited (Figure 2F). In addition, the h-pruneΔ mutant is not activated by the Mg^{2+} ions as well as the wild-type protein (Figure 2F), thus indicating that the motif III, modified in h-pruneΔ mutant, is necessary for phophodiesterase activity. In conclusion, we show here that h-prune cAMP-PDE activity is influenced positively by the Mg^{2+} ion concentration.

Stable breast MDA h-prune clones and correlation to cellular motility

To study the h-prune function in regulating nm23-H1 antimotility and suppressor metastasis activities, we have taken advantage of the breast cancer cellular models MDA-C100 and H1-177 (Hartsough et al., 2001; Mao et al., 2001; Tseng et al., 2001).

We produced several stable clones overexpressing the h-prune cDNA (clones #3 and #4), the h-pruneΔ cDNA (clones #10 and #11), the h-prune4DΔ cDNA (clones #19 and #20), and the PDE5A cDNA (clones #14 and #16) in MDA-C100 cells. We stabilized the h-prune cDNA in MDA-H1-177 overexpressing nm23-H1 (clones #7 and #8), in MDA overexpressing nm23H1-P96S (clones #4 and #5), and in MDA overexpressing nm23H1-S120G (clones #2 and #3). Several of these clones were characterized to determine the expression level of h-prune mRNA using real-time PCR analysis by TaqMan technology (Figure 3A). We selected four clones for their level of mRNA expression by quantitative analysis and copy number extrapolation, as compared to gene reference targets (GAPDH) (Figure 3B). In addition, Western blot analyses were performed to identify the expression levels of the h-prune, nm23, and PDE5A proteins (Figure 3C). The stable clones produced were then assayed for cellular motility using the Trans-well cell culture chambers (Freije et al., 1997a). Six independent clones (MDA-C100; MDA-prune clones #3 and #4; MDA-H1-177-prune clones #7 and #8; MDA-H1-177) were assayed. Overall, the MDA-prune clones have a 2-fold increase in motility as compared to the control cell line MDA-C100 (Figure 3D). The values observed for the MDA-H1-177-prune clones are increased 2.2-fold as compared to the cell line MDA-H1-177, overexpressing nm23-H1 alone (Figure 3D). The clone MDA-H1-177 value observed is reduced by a mean of almost 40% compared to the MDA-C100 cell line, as it was described previously (Hartsough et al., 2001), thus confirming the role of nm23-H1 in the inhibition of cellular motility.

In order to study the contribution of h-prune PDE activity to cell motility, we performed the motility assay on MDA-C100, MDA-H1-177, MDA-prune (clones #3 and #4), MDA-pruneΔ (clones #10 and #11), and MDA-prune4DΔ (clones #19 and #20).

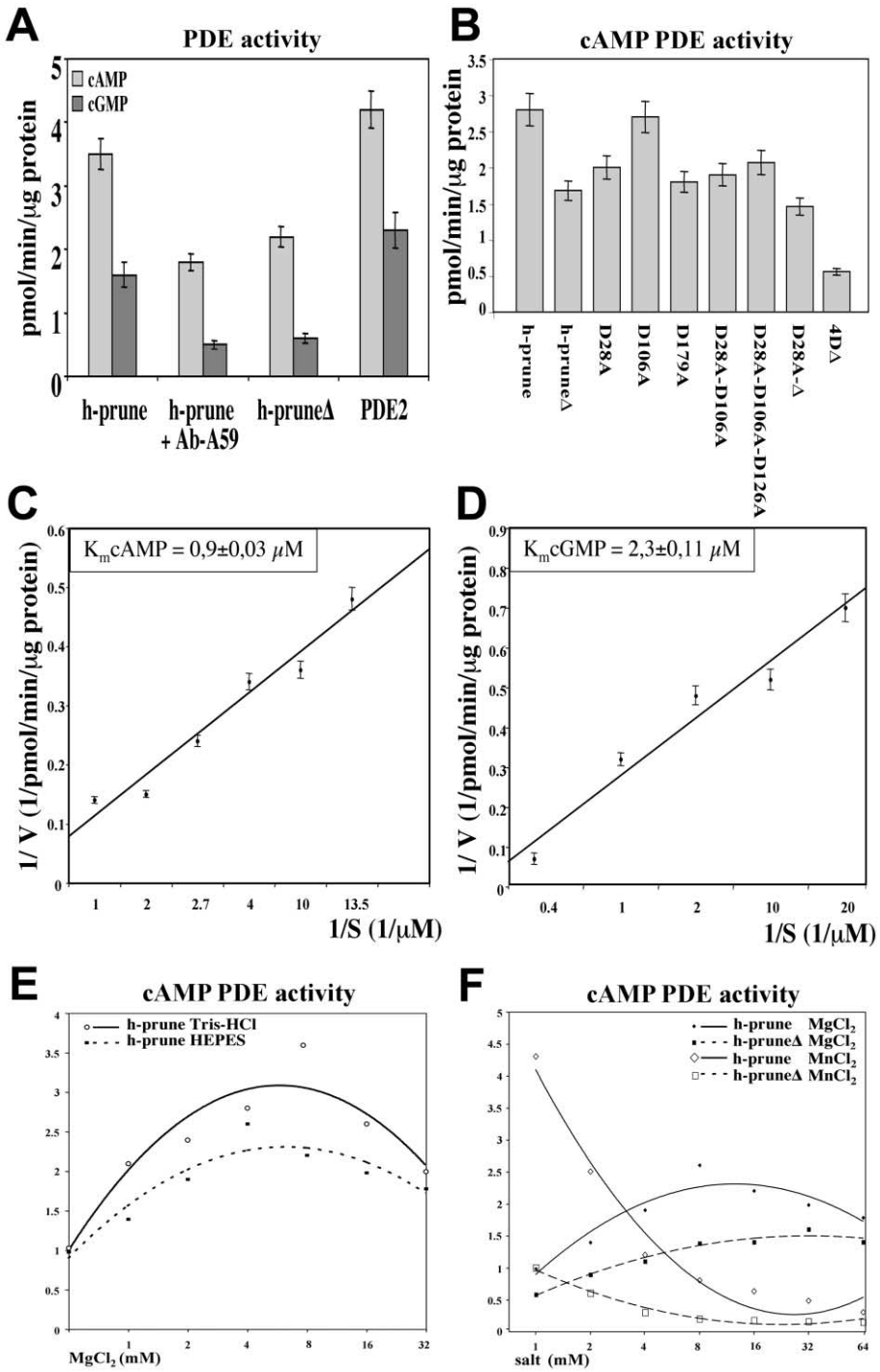

Figure 2. Identification of h-prune PDE activity

A: H-prune PDE activity for cAMP and cGMP as substrates. Negative controls, h prune preincubated with specific antibody (A59), h-pruneΔ, a mutant protein in the motif III characteristic of DHH protein family ($p < 0.03$). Positive control, purified PDE2 protein.

B: Mutational analyses in the potential catalytic site of h-prune protein. Single and multiple mutations in all the amino acids of the DHH characteristic motifs and their cAMP-PDE activities are reported in the histogram ($p < 0.03$).

C and D: Lineweaver-Burk plots to determine K_m and V_{max} for both cAMP and cGMP as substrate, respectively.

E: cAMP-PDE activity measured in the presence of two different buffers at increasing concentrations of Mg^{2+}.

F: cAMP-PDE activity measured in the presence of increasing concentrations of Mg^{2+} (black points) or Mn^{2+} (white points). Activity plots of both h-prune (solid lines) and h-pruneΔ (scattered lines) are shown. In all the assays presented, the activities values are arithmetical means ± SD for five independent assays, each conducted in triplicate.

We chose these mutants because of their different abilities to influence h-prune PDE activity. Compared to MDA-prune stable clones (Figure 3E), we observed a 40% decrease in cell motility in MDA-pruneΔ clones and almost a complete decrease (90%) in MDA-prune4DΔ. To verify whether h-prune PDE activity contributes alone to cell motility in breast cancer cell lines, we tested the clones overexpressing a well-characterized PDE (PDE5A) in MDA-C100 (MDA-PDE5A clones #14 and #16). No increase in cell motility was observed in both PDE5A overexpressing clones (Figure 3E), thus indicating that only the h-prune PDE activity is able to induce cell motility in this conventional cellular model.

In addition, it has been reported (MacDonald et al., 1996; Freije et al., 1997a) that the nm23H1-S120G (a mutant showing an impaired interaction with h-prune) (Reymond et al., 1999) and nm23H1-P96S (a mutant that retains its ability to bind h-prune) proteins are able to induce cellular motility. We investigated the role of h-prune in cellular motility overexpressing mutants alone and together with h-prune and correlated this to cellular motility.

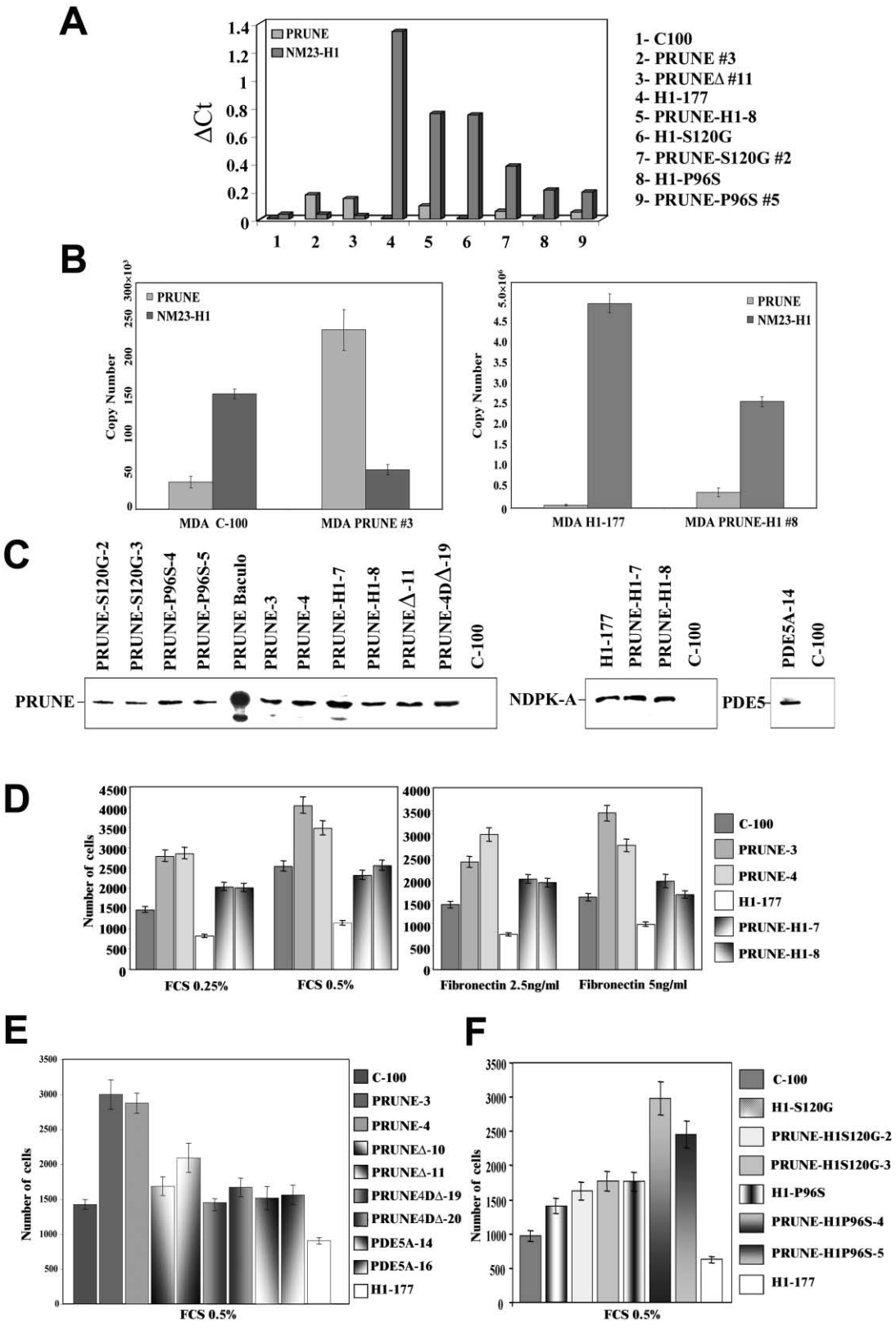

Figure 3. Stable clone analyses and in vitro motility assay

A: mRNA expression of *h-prune* and *nm23-H1* genes by real-time PCR quantitative analysis. Relative ΔCt values are indicated. Histograms and copy numbers were extrapolated by real-time software analysis.

B: Real-time mRNA detection performed with TaqMan technology. Copy number of stable clones are represented. The mRNA copy number measured values are arithmetical means ± SD for three independent assays, each conducted in triplicate.

The MDA-nm23H1-S120G-prune clones show an almost 60% increase in motility as compared to the MDA-C100 control cell line, while the MDA-nm23H1-P96S-prune clones show a 200% increase in motility when compared to MDA-C100 cells (Figure 3F).

In conclusion, our findings indicate that overexpression of h-prune in MDA-C100 cells increases their cellular motility. H-prune is able to revert the antimotility effect of nm23-H1, thus promoting cellular motility. This effect is not observed when h-prune is overexpressed in the presence of the impaired interacting nm23H1-S120G mutant, thus postulating a role of nm23-H1-h-prune complex in increasing cellular motility.

In vitro and in vivo h-prune PDE activity

Considering that h-prune and nm23-H1 physically interact (MacDonald et al., 1996), we investigated whether nm23s may influence the PDE activity of h-prune and the biochemical significance of the nm23-h-prune interaction. This was achieved by preincubating nm23-H1 with h-prune purified protein and measuring the cAMP-PDE activity in vitro. H-prune PDE activity showed up to a 2-fold increase in the presence of nm23-H1 over the control (Figure 4A). In addition, to verify that this increased activity was due to a physical interaction, we tested different nm23 mutants. The noninteracting mutant nm23H1-S120G (Figure 4A) was not able to increase h-prune PDE activity. In contrast, the interacting mutant nm23H1-P96S increased h-prune PDE activity almost like the wild-type nm23-H1 did, although to a lesser extent. This is possible because of the lower binding affinity to h-prune previously reported (Reymond et al., 1999). As a further control experiment, we tested h-pruneΔ PDE activity in the presence of nm23-H1 protein. These two proteins do not interact by coimmunoprecipitation assays (data not shown). Indeed, there is no increase in h-pruneΔ PDE activity measured (Figure 4A). Altogether, these results demonstrate a correlation between the direct physical interaction of h-prune and nm23-H1 and the increase of h-prune PDE activity. Furthermore, each stable clone used in the motility assay was analyzed for specific h-prune cAMP-PDE activity on immunoprecipitated protein (Figure 4B). Through these analyses, the MDA-prune clones have an 8-fold increase of cAMP-PDE activity as compared to the MDA-C100 clone. Instead, the MDA-pruneΔ clones have a 0.5-fold decrease of cAMP-PDE activity as compared to the MDA-prune clones, and this correlates to their cell motility properties (Figure 4B). In addition, we found that h-prune PDE activity in MDA-prune compared to double stable clones MDA-H1-177-prune is increased 1.4-fold (Figure 4B). These results show a direct correlation of h-prune PDE activity to cell motility. Further-

A

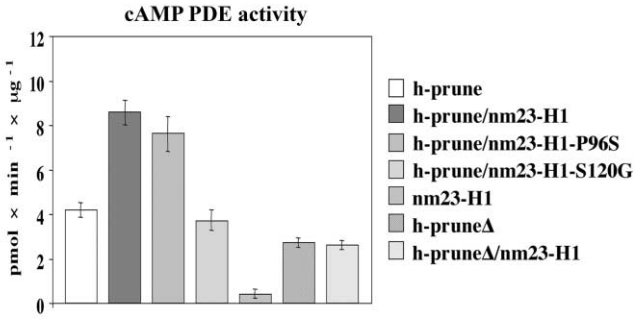

B

Clone name	h-prune PDE activity (pmol×min^{-1}×µg^{-1})	Motility (number of cells)
MDA C-100	3.8±0.7	1548±84
MDA H1-177	2.2±0.4	928±73
MDA PRUNE #3	35±5.3	2812±294
MDA PRUNE #4	28.7±2.5	3272±271
MDA PRUNEΔ #10	16.8±1.2	1682±64
MDA PRUNEΔ #11	14.6±0.9	2087±97
MDA PRUNE-H1 #7	18.8±2.6	2048±93
MDA PRUNE-H1 #8	22±4.2	2006±87
MDA H1S120G	2.4±0.8	1328±54
MDA PRUNE-H1S120G #2	4.4±1.6	1624±89
MDA PRUNE-H1S120G #3	5.3±1.4	1767±108
MDA H1P96S	3.0±0.3	1742±38
MDA PRUNE-H1P96S #4	19.2±0.3	2982±184
MDA PRUNE-H1P96S #5	11.6±0.4	2448±143

Figure 4. In vitro and in vivo h-prune PDE activity

A: H-prune and h-pruneΔ cAMP-PDE activity in the presence of nm23 proteins ($p < 0.03$). Negative control, nm23-H1 and h-pruneΔ purified proteins. Positive control, h-prune purified protein. The activities values are arithmetical means ± SD for five independent assays, each conducted in triplicate.
B: H-prune PDE activity measured as pmol × min^{-1} × µg^{-1} on whole protein cell lysates immunoprecipitated with the specific anti-h-prune antibody (A59) at 4°C overnight. The activity values are arithmetical means ± SD for five independent assays, each conducted in triplicate. Cellular motility was measured after attraction by 0.5% FCS, as the number of cells subjected to motility and counted under the microscope. Cell motility measured values are arithmetical means ± SD for three independent assays, each conducted in duplicate.

C: Western blot analyses using Abs specific for h-prune, nm23-H1, and His-tag (for PDE5A) indicate the amount of proteins expressed in each individual cell clone. Twenty micrograms total protein cell lysate were loaded in each lane. Purified baculovirus h-prune protein was used as a positive control.
D: Cellular motility of MDA C-100 (control cell line), MDA H1-177, MDA-prune, and MDA-H1-177-prune cell lines, overexpressing *h-prune* (clones #3 and #4) alone or *h-prune* and *nm23-H1* (clones #7 and #8), respectively, was measured after attraction by two different chemoattractors as the number of cells subjected to motility and counted under the microscope ($p < 0.05$).
E: Cellular motility of MDA-C100 (control cell line), MDA-prune (clones #3 and #4), MDA-pruneΔ (clones #10 and #11), MDA-prune4DΔ (clones #19 and #20), MDA-PDE5A (clones #14 and #16), and MDA-H1-177 cell lines was measured after attraction by 0.5% FCS as the number of cells subjected to motility and counted under the microscope (MDA-C100/MDA-prune $p < 0.01$; MDA-pruneΔ/MDA-prune $p < 0.025$; MDA-prune4DΔ/MDA-prune $p < 0.001$; MDA-prune/MDA-PDE5A $p < 0.004$).
F: Cellular motility of MDA-C100 (control cell line) and MDA-nm23H1-S120G, MDA-nm23H1-S120G-prune (clones #2 and #3), MDA-nm23H1-P96S, MDA-nm23H1-P96S-prune (clones #4 and #5) cell lines, overexpressing nm23-H1 mutants alone or with h-prune was measured after attraction by 0.5% FCS as the number of cells subjected to motility and counted under the microscope (MDA-C100/MDA-nm23H1-S120G-prune $p < 0.008$; MDA-C100/MDA-nm23H1-P96S-prune $p < 0.005$; MDA-nm23H1-P96S-prune/MDA-nm23H1-S120G-prune $p < 0.003$). All the motility assay histograms represent the number of cells and the arithmetical means ± SD for three independent experiments performed in duplicate.

more, the MDA-nm23H1-S120G-prune clones have a 3-fold decrease of h-prune PDE activity as compared to the MDA-nm23H1-P96S-prune clones, thus implying a direct correlation between h-prune cAMP-PDE activity, cellular motility, and protein-protein interactions. In conclusion, we noted a direct correlation between h-prune PDE function and protein-protein interactions, resulting in a significant influence on cellular motility.

PDE inhibitor studies of h-prune and influence on cellular motility

To identify the physiological role(s) of h-prune cAMP PDE activity in the cell, we tested a panel of selective PDE inhibitors and verified whether any were affecting h-prune protein activity. The ability of h-prune to hydrolyze cAMP was inhibited selectively by dipyridamole (already known to act against PDE5, PDE6, PDE9, PDE10, and PDE11). The IC_{50} measured for dipyridamole inhibition of h-prune PDE activity was 0.78 ± 0.05 μM, and this value is lower (higher specificity) if compared to the other dipyridamole selective PDEs (PDE5, PDE9, PDE10). Only PDE6 and PDE11 have a lower IC_{50} compared to h-prune IC_{50} value (Figure 5A). H-prune was also moderately sensitive to IBMX (IC_{50}: 40.2 ± 0.8 μM), a nonselective specific PDE inhibitor, and to vinpocetine (IC_{50}: 22.3 ± 1.1 μM), a PDE1C-specific inhibitor. Several other inhibitors used in this study did not affect h-prune hydrolysis of cAMP, even when applied at 100-fold higher concentrations than those defined as their IC_{50} values measured against other PDEs. The results of the inhibitor studies are summarized in Figure 5A.

The data presented above were further verified in the MDA-MB-435 breast cancer cell line in order to study the physiological inhibition in vitro. We choose to use h-prune overexpressing MDA clones and, as additional controls, MDA-pruneΔ clones because of a partial reduction (40%) of h-prune PDE activity, as discussed above (Figures 2A and 2B), to verify the extent to which dipyridamole was able to inhibit their activities and correlate them to cellular motility. Both the MDA-prune and pruneΔ clones were incubated with dipyridamole (8 μM, a 10-fold higher concentration with respect to its IC_{50}) for 24 hr to obtain the complete enzyme inactivation, and then the motility assay was repeated as described above. After treatment with dipyridamole, the MDA-prune and MDA-pruneΔ clones showed an average reduction of 40% and 20% in motility, respectively, showing that the inhibitor acts against h-prune PDE activity, thus inferring a substantial decrease in cellular motility (Figure 5B). These results are of pharmacological impact because of partial success in the use of dipyridamole in combination with other drugs in clinical trials in breast (Budd et al., 1990, 1994) and gastric and intestinal carcinoma (Hejna et al., 1999).

A

Inhibitor	Selective for PDE type	IC_{50}μM	h-prune IC_{50}μM
Cilostamide	PDE3	0.05	>100
Dipyridamole	PDE5/6/9/10/11	0.9/0.38/4.5/1.1/0.37	0.78±0.05
IBMX	nonselective	2-59	40.2±0.8
Milrinone	PDE3	1.3	>100
Rolipram	PDE4	2.0	>100
Vinpocetine	PDE1C	8.1	22.3±1.1
Zaprinast	PDE1/5/6	6.9/0.76/0.15	>100
Sulindac	cGMP PDEs	n.a.	>100

B

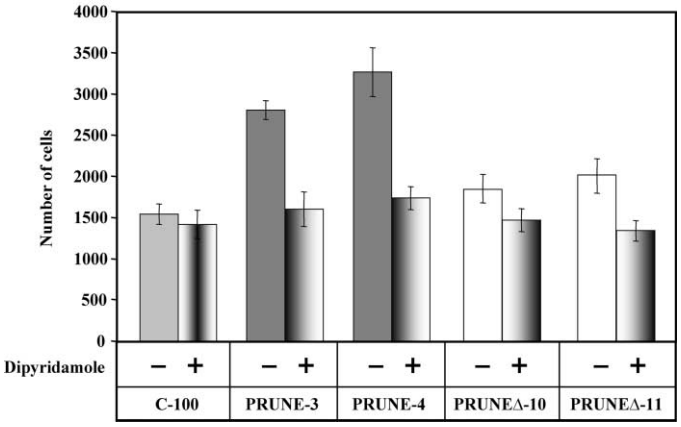

Figure 5. PDE inhibitor studies and cellular motility

A: Eight inhibitors were tested for h-prune PDE activity. In second and third, columns for each inhibitor are listed for the specific or selective PDEs and their respective IC_{50} values. On the last column, h-prune IC_{50} is reported for the most sensitive compounds: dipyridamole, IBMX, and vinpocetine. The activity values presented are arithmetical means ± SD for three independent assays, each conducted in triplicate.

B: MDA-C100 (control cell line), MDA-prune (clones #3 and #4), and MDA-pruneΔ (clones #10 and #11) cell lines were treated with 8.0 μM dipyridamole for 24 hr. Cellular motility was measured after attraction by 0.5% FCS as visualized and counted under the microscope (MDA-prune clones #3 and # 4, $p < 0.04$). Motility assay histograms represent the number of cells as arithmetical means ± SD for three independent assays, each conducted in duplicate.

Breast carcinoma study on metastases-affected patients

To verify the oncogenic role of h-prune in vivo, we have randomly selected 59 cases for which metastasis has been reported (TxNxM1 according to TNM classification which describes the anatomical extent of disease). Analysis was performed on a tissue multiple array (TMA) containing primary tumor tissue cases that showed metastasis at the time of diagnosis or during follow-up (at least 5 years of follow-up; date of diagnosis: 1992–1997). FISH analyses, using a PAC containing h-prune (279-H19) as probe, revealed 22 out of 59 (37%) tumor cases with trisomy or higher copy number, indicating amplification of the h-prune genomic region (a normal diploid signal was found using the centromeric control probe), whereas only disomy and definitively no amplification was observed in a total of 55 cases analyzed using a PAC containing nm23-H1 as probe (Figure 6A). In addition, immunohistochemical analyses on TMA were performed using two antibodies (A59, K73) that recognize h-prune and nm23-H1, respectively. FISH and immunohistochemical analyses of normal as well as nonmetastatic cancer tissues were reported (see the Supplemental Data at http://www.cancercell.org/cgi/content/full/5/2/137/DC1).

According to immunohistopathology grading, all 22 cases (37%) with cytogenetic amplification of the h-prune chromosomal region also presented high h-prune protein expression in contrast to the low or moderate expression level of nm23-H1, thus suggesting that about one third of breast metastasis formation may be due to both h-prune amplification and overexpression with concurrent diminished level of the nm23-H1 sup-

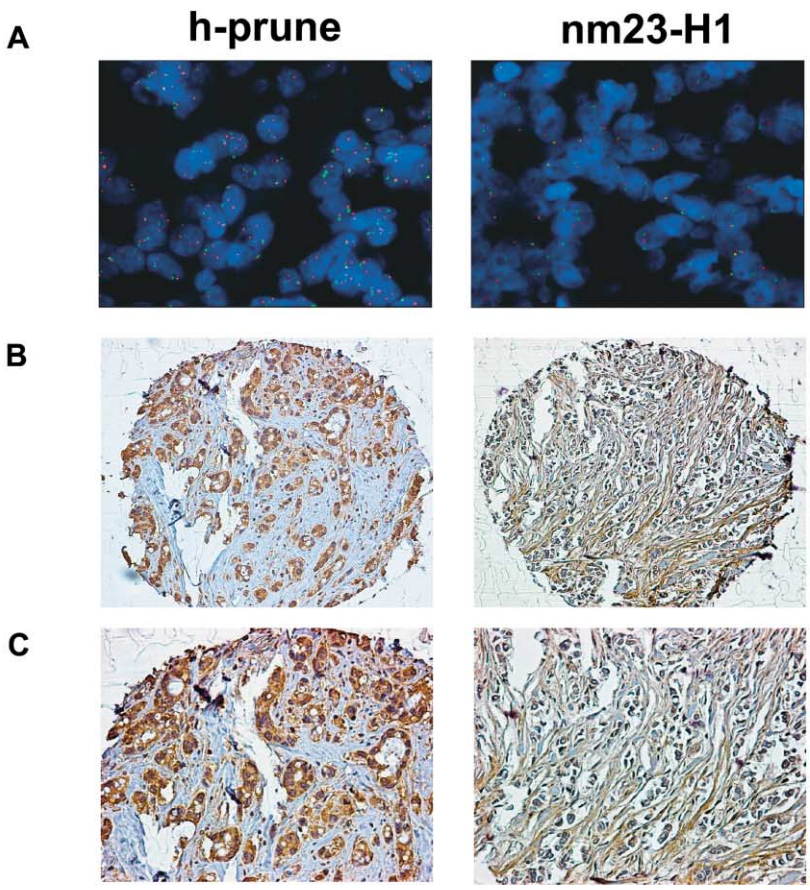

Figure 6. In vivo analysis of breast metastasis-associated tumors

A: FISH analysis on multiple tissue array (MTA) shows copy number amplification of h-prune (left) and an example of nm23-H1 (right). FISH results were obtained using PAC 279-H19 (red, left panel), PAC nm23-H1 (red, right panel), and the control pUC177 (green, both panels) as probes.

B and C: 100× and 200× magnification of immunohistochemical analysis on two tumors cohorts with high expression (+++) of h-prune (left) compared to a very moderate and low (0/+) nm23-H1 expression (right).

D: Summary table of both FISH and IHC analyses performed on 59 TxNxM1 breast cancer cases.

D

		FISH analysis			
		PAC h-prune (1q21.3)		PAC nm23-H1 (17q21)	
Immunohistochemistry (IHC)	**IHC grade**	Disomy	Trisomy or more	Disomy	Trisomy or more
h-prune	+++/++	**7** (12%)	**22** (37%)		
	+/0	**30** (51%)			
nm23-h1	+++/++			**1** (2%)	
	+/0			**54** (98%)	
TNM_1 cases analyzed		**59**		**55**	

pressor metastasis function. In addition, seven cases (12%) do not present h-prune amplification but possess high h-prune protein level while nm-23H1 level is low (Figure 6D). This suggests the presence of an alternative mechanism of h-prune overexpression independent from gene amplification.

For the remaining 37 out of 59 (63%) cases with TxNxM1 tumors, we can hypothesize the involvement of an alternative pathogenetic pathway that is responsible for metastasis formation. These data indicate a metastasis-promoting role of h-prune protein in breast carcinoma.

Discussion

Structural analyses based on the two proteins belonging to the DHH superfamily, namely the RecJ nuclease and the inorganic pyrophosphatase, suggested that h-prune is likely to possess a metal ion-dependent phosphoesterase activity. Because of the DHH family structural analysis and evolutionary protein folding studies of phosphoesterases, we demonstrated that mammalian h-prune possesses a cyclic nucleotide phosphodiesterase activity. Since h-prune interacts with the nm23-H1 isoform that has NDPK activity, which is known to function on nucleotides, we focused our attention on the characterization of the cyclic nucleotides phosphodiesterase activity and its role in cellular signaling. The h-pruneΔ mutant that contains substitutions in the conserved motif III of the DHH family shows a reduction of the PDE activity (Figures 2A, 2B, and 2F). Mutation analysis at single and multiple sites indicate that only mutations in histidine (127), argine (128), and proline (129) of motif III and in the aspartic acids D28, D126, and D179 present, respectively,

in motif I, III, and IV, were found to substantially affect the h-prune PDE activity, most likely indicating their involvement in the h-prune PDE catalytic site.

The conserved motif III region is responsible for the binding of Mg^{2+} ions as predicted by protein modeling (Figure 1B), and, in addition, in an in vitro functional assay, we observed that h-prune is also able to function in the absence (Figure 2E) or at low concentrations of metal ions (Figure 2F).

We have previously demonstrated that h-prune and the nm23s protein levels are unbalanced in sarcoma and breast carcinoma tumors, suggesting that h-prune may negatively regulate nm23-H1 antimetastatic function. An increase in h-prune expression is a direct correlation with the aggressiveness of those tumors and cancer progression (Forus et al., 2001). Since several reports have postulated that the antimetastatic activity of nm23-H1 is independent of the NDPK activity (Wagner et al., 1997), we investigated what influence h-prune has on cellular motility, which represents one of the first cellular functions to be acquired by the cancer cell to migrate away from the primary tumor site.

In order to confirm that h-prune PDE activity is directly involved in these phenomena, we overexpressed h-prune, h-pruneΔ, and h-prune4DΔ in a breast cancer model and observed that overexpression of the wild-type protein induces cell motility, while a decrease of its PDE function (h-pruneΔ, h-prune4DΔ) corresponds to a decrease in cell motility. Indeed, we observed an 80% reduction of PDE activity for the mutant h-prune4DΔ, and overexpression in MDA clone shows no significant increase in cell motility, thus excluding that other potential h-prune activities are responsible for increasing motility. To date, even though no other intracellular characterized PDEs have been associated with cell migration, we investigated whether the increment of PDE activity in MDA stable clones might contribute to cell motility. In order to verify this, we overexpressed PDE5A in the same cellular model and tested for cell motility. PDE5A, chosen for its sensitivity to dipyridamole (IC_{50} 0.9 μM), did not affect MDA breast cell motility, thus indicating that only h-prune PDE function is responsible for increasing cell motility in breast cancer cells.

In addition, we observed that overexpression of h-prune in a high nm23-H1 expression background displays a decreased motility phenotype and a lower h-prune PDE activity compared to the cells overexpressing h-prune alone. Although h-prune PDE activity is increased in vitro upon interaction with nm23-H1 (Figure 4A), this effect is not observed in vivo. These phenomena can be explained by the presence of a high amount of nm23-H1 in MDA-H1-177-prune as compared to MDA-prune clones (Figure 3B). This can negatively influence the prune-nm23H1 complex formation, which might depend on the presence of different oligomeric and/or posttranslationally modified nm23-H1 forms (for example, serine phosphorylation) (Steeg, 2003).

In order to test the hypothesis that the negative regulation of h-prune on the nm23 antimetastatic function is due to an increase in PDE activity as a result of the protein-protein interaction, we investigated what effect two nm23-H1 mutants hold on h-prune PDE activity. These protein mutants are nm23H1-P96S, which is able to physically interact with h-prune, and nm23H1-S120G, which does not interact with h-prune (Reymond et al., 1999). Both mutants transfected in breast cancer cells (MDA-435) are able to suppress the endogenous antimotility effect of the nm23-H1 wild-type protein (Freije et al., 1997a; MacDonald et al., 1996). Additionally, we show that breast cancer cells overexpressing h-prune in a high nm23-H1-S120G expression background have lower cellular motility in comparison to cells overexpressing h-prune in a high nm23-H1-P96S background, thus further indicating that the physical interaction between these two proteins may be responsible for the motility-promoting role. Furthermore, the h-prune-nm23-H1-S120G clone has almost 66% lower PDE activity compared to the PDE value observed in the clone overexpressing both h-prune and nm23-H1-P96S (Figure 4B), thus definitively indicating a correlation between protein-protein interaction, h-prune cAMP-PDE activity, and cellular motility effects.

In order to understand whether any known PDE inhibitors were able to function selectively against h-prune PDE activity, we tested a panel of eight PDE inhibitors and found that dipyridamole was able to inhibit h-prune PDE activity with a significant IC_{50} value. In addition, the use of dipyridamole severely reduced the motility of the stable h-prune breast clones and, to a lesser extent, the h-pruneΔ overexpressing clones (Figure 5B). Although dipyridamole might not be the most effective h-prune cAMP PDE inhibitor, and further experiments have to be performed to identify a new highly specific compound, these findings are of pharmacological interest. It is common opinion that anticoagulants such as dipyridamole and similar drugs exert their function by interfering with the blood-clotting pathway activation through inhibition of adhesion of metastatic cells to capillary walls. These results are an added value to those presented in vivo (Haaz et al., 1996) describing the positive effect of dipyridamole and fluorouracil (FU) combination in chemotherapy and in several clinical trials. Examples are in breast (Budd et al., 1994) and gastric and intestinal carcinoma (Hejna et al., 1999). Dipyridamole in combination with protease inhibitors, interferon, and 5-fluoroUracil inhibits metastasis formation. In view of the results reported here, we believe that the use of dipyridamole might hold promise for the prevention and treatment of breast metastases spread, and a large controlled investigation study might provide further evidence.

Moreover, we confirmed in vivo the data observed on cellular motility activation in vitro, using a significant number of breast cancer tissues from TxNxM1 patients. In 59 tumors from cases presenting distal metastasis, *h-prune* was found amplified in copy number and overexpressed in 22 cases (37%), whereas *nm23-H1* was found expressed at lower levels in all analyzed cases (Figures 6B–6D). The data presented indicate that h-prune upregulates genes involved in metastasis, and its activity in vivo increases the risk of more aggressive tumor behavior, contributing negatively to the clinical outcome in breast cancer patients. The results reported here have important pharmacological consequences, as drugs that are able to selectively inhibit h-prune PDE activity can be used in the treatment of breast carcinoma in order to block h-prune prometastasis malignancy function. Furthermore, we have analyzed by array expression analyses and validated by real-time PCR 11 genes involved in oncogenesis and metastasis processes whose expression was found to be altered in breast MDA-H1-177-prune clone #8 compared to MDA-H1-177 clone. The results presented are additional evidence of the aggressiveness and metastatic potential of the MDA breast cancer cell line upon h-prune overexpression (see the Supplemental Data at http://www.cancercell.org/cgi/content/full/5/2/137/DC1).

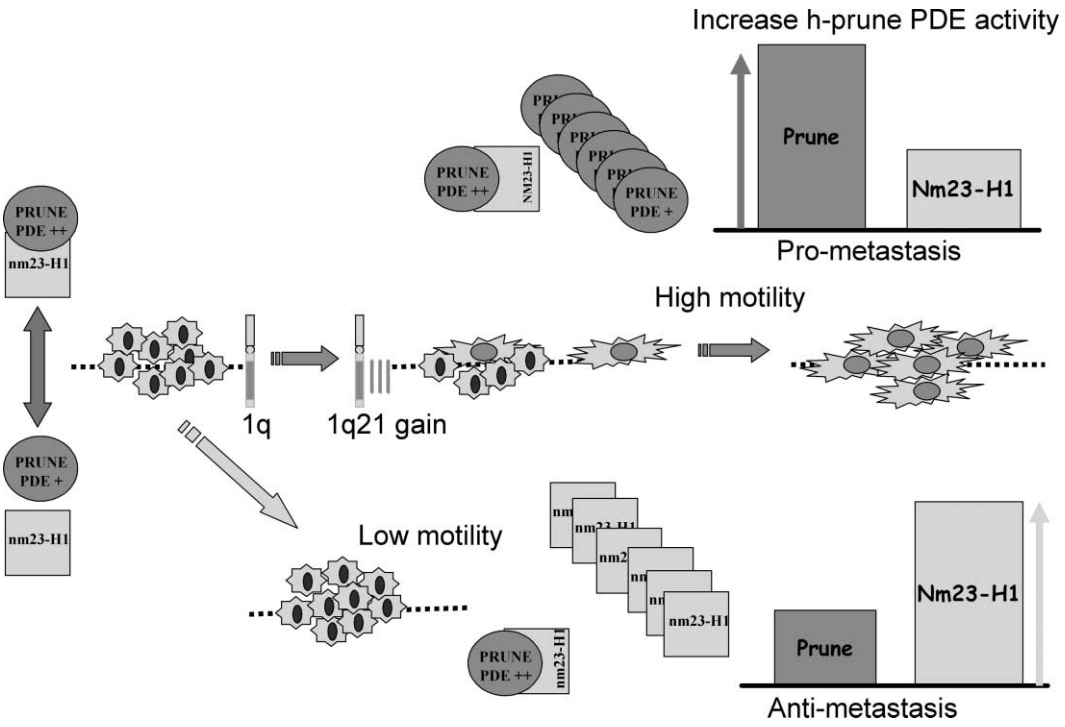

Figure 7. A model representing h-prune prometastatic function in breast cancer

In the cytoplasm of the cell, h-prune and nm23-H1 may exist in free forms and/or in a protein complex. In a cancer-committed cell, chromosomal 1q gain occurs, increasing *h-prune* copy number and protein content, thus influencing cellular motility and h-prune PDE activity and promoting cancer metastasis. In contrast, the overexpression of nm23-H1 in breast cancer cells translates in reducing cellular motility and enhancing its potential to suppress metastases formations.

Overall, these experiments shed light on the role of h-prune in the promotion of cellular motility and metastases negatively influencing the nm23-H1 antimetastatic function. Our model of the role of h-prune in cancer progression invokes, in general, its amplification in tumor cells. The amplification leads to an increased h-prune PDE activity in the cytoplasmic compartment, thus negatively influencing the suppressor of metastasis function of the nm23s. The activation of the h-prune PDE activity is due to a physical interaction with the nm23-H1 protein. The complex formation results in a substantial decrease of the level of free nm23-H1 forms, thus influencing cell proliferation, cellular motility, and metastatic processes (Figure 7).

How the h-prune-nm23 protein complex influences nm23-H1 metastasis suppressor function and apoptosis by promoting terminal differentiation and malignancy is not yet known. These questions and their following experimental plans will be aims of future research efforts.

Further specific investigations to address the biological functions of h-prune and nm23 in other model organisms should help uncover the potential significance of this pathway in metastasis as well as in cellular motility and development.

Experimental procedures

Protein sequence analysis

The nonredundant database of protein sequences at the National Center for Biotechnology Information (NIH, Bethesda, MD) was iteratively searched using the PSI-BLAST program (Altschul et al., 1997). Multiple alignments of protein sequences were constructed using the T-coffee program (Notredame et al., 2000) and corrected on the basis of PSI-BLAST results. Phylogenetic trees were constructed using the Fitch program of the Phylip and the ProtML program of the Molphy package. Homology modeling of protein structures was performed using the SWISS-MODEL server (Guex and Peitsch, 1997). The target was threaded to the template using the SWISS-PDBviewer software, and the alignment with the template was manually adjusted to minimize the clashes of the protein backbone. The energy minimization was carried out using the GROMOS program that uses a Sippl-like force field. The ribbon diagrams of the structures were generated using the MOLSCRIPT program.

Cell culture

HEK-293 and MDA-MB-435 cells were cultured in Dulbecco's modified Eagle's medium supplemented with 10% fetal bovine serum, 100 Units/ml penicillin, and 100 μg/ml streptomycin at 37°C with 5% CO_2.

Protein expression and purification in Baculovirus

Protein expression was performed using Baculovirus Expression System (Invitrogen). In brief, the cDNAs coding for *h-prune, nm23-H1*, and the *nm23-H1* (MacDonald et al., 1996) and *h-prune* mutants h-pruneΔ, D28A, D106A, D179A, D28A-D106A, D28A-D106A-D126A, D28A-Δ, and 4DΔ (D28A-D106A-Δ-D179A) were subcloned into the EcoRI/XhoI-digested pFastBac-Hta vector. In order to produce the h-prune mutants cDNA, site-directed mutageneses of the h-prune construct were performed using the QuikChange III Kit (Stratagene) according to the manufacturer's instructions (see the Supplemental Data at http://www.cancercell.org/cgi/content/full/5/2/137/DC1). Virus infection and purification conditions are described in Garzia et al. (2003). Histidine-tagged h-prune and h-pruneΔ were further purified on a MonoQ HR 5/5 column (Amersham) using 10 mM Tris-HCl (pH 8.0) buffer. Column elution was performed with a linear gradient from 0 to 0.8 M NaCl over 20 min and at a flow rate of 1 ml/min. The fractions were further dialysed against 10 mM Tris-HCl (pH 8.0) buffer, and tested for activity. The purity of isolated proteins was measured by electrophoresis SDS page analysis.

Identification and characterization of the h-prune phosphodiesterase activity

PDE activity was measured by a cAMP/cGMP detection assay, as described by Fisher et al. (1998), and with a scintillation proximity assay (Amersham-Pharmacia Biotech). Samples were diluted as required and incubated at 30°C in 100 μl assay buffer (50 mM Tris-HCl [pH 7.4], 8.3 mM $MgCl_2$, 1.7 mM EGTA) containing the desired concentrations of cAMP or cGMP as substrate (3:1 ratio unlabeled to ^{3}H-labeled). All reactions, including buffer-only blanks, were conducted in triplicate and allowed to proceed for an incubation time giving <25% substrate turnover (empirically determined). Reactions were terminated by adding 50 μl Yttrium silicate SPA beads (Amersham). Enzyme activities were calculated for the amount of radiolabeled product detected according to the manufacturer's protocol. As negative controls, we used h-prune preincubated with the A59 polyclonal antibody, raised against the motif III region (Apotech Corporation, CH) and h-pruneΔ mutant. In particular, for h-prune and h-prune mutants PDE activity, 200 ng of purified enzymes were incubated for 10 min at 30°C. Lineweaver-Burk plots with K_m and V_{max} values were determined by measuring hydrolysis with a range of substrate concentrations (0.05–10.0 μM) and a fixed amount of diluted enzyme over a time course of 5–40 min. Initial rates were calculated at each substrate concentration and plotted against substrate concentration, from which the kinetic parameters were determined. To study the influence of different buffers and of nm23 activity on h-prune PDE activity and to perform inhibitor studies, we modified PDE assays as described in Supplemental Data (http://www.cancercell.org/cgi/content/full/5/2/137/DC1).

In vitro cell motility assay

Stable MDA clones overexpressing h-prune, h-pruneΔ, h-prune4DΔ, and human PDE5A were produced and analyzed as described in Supplemental Data (http://www.cancercell.org/cgi/content/full/5/2/137/DC1). The control MDA-C100 breast cancer cell line was used in the "cell motility" assay, as described (Leone et al., 1993a, 1993b), with the cell line overexpressing nm23-H1 (MDA-H1-177), which shows an inhibition of metastasis processes in vivo. Cellular motility was determined using the transwell technology (6-well, Corning-Costar) using 0.25%, 0.5% FCS, 2.5, and 5.0 ng/ml fibronectin (Sigma) final concentrations as chemoattractants (for details, see Supplemental Data). The in vitro h-prune inhibition motility assay was performed as follows. The MDA-prune (clones #3 and #4) and MDA-pruneΔ (clones #10 and #11) were incubated with dipyridamole (8 μM, a 10-fold higher concentration with respect to its IC_{50}) for 24 hr to obtain the complete enzyme inactivation, and then the motility assay was repeated as described above.

Statistical analyses

All the assays, including PDE activity and cellular motility, were validated using the unpaired t test method available at http://www.graphpad.com/quickcalcs/index.cfm.

FISH and IHC analyses—tumor case collection and TNM selection

For FISH and IHC analyses, tumor case collection, and TNM selection, see the Supplemental Data (http://www.cancercell.org/cgi/content/full/5/2/137/DC1).

Acknowledgments

Our special thanks go to Dr. P.S. Steeg for sharing the MDA-C100, MDA-H1-177, MDA-nm23H1-P96S, and MDA-nm23H1-S120G clones; the DNA TIGEM-IIGB Sequencing Core for developing sequencing reactions; Dr. Keni Omori for PDE5A gene construct; the MicroArray Core facility and Dr. Cocchia for help on data mining; Dr. Budroni for breast data collection analysis; Drs. Beavo, Iolascon, Santoro, and Venkitaraman for critical discussions of the manuscript; and Drs. Meroni and Diez-Roux for supportive ideas on project development. This work was supported by an AIRC-FIRC Research Fellowship to A.D., a Molecular Oncology and Pharmacology PhD program (University of Ferrara, Italy) to V.A., a 2002 AIRC-FIRC grant (G.P, M.Z.), a Compagnia San Paolo Torino 2002 grant (M.Z.), a Regione Autonoma della Sardegna 2001-03 grant (A.C., G.P.), a FIRB-MIUR-RBAU01RW82 grant (M.Z.), and a 2001 TIGEM-Telethon Regione Campania grant (M.Z.).

Received: June 26, 2003
Revised: November 1, 2003
Accepted: November 24, 2003
Published: February 23, 2004

References

Ahn, S., Milner, A.J., Futterer, K., Konopka, M., Ilias, M., Young, T.W., and White, S.A. (2001). The "open" and "closed" structures of the type-C inorganic pyrophosphatases from Bacillus subtilis and Streptococcus gordonii. J. Mol. Biol. *313*, 797–811.

Altschul, S.F., Madden, T.L., Schaffer, A.A., Zhang, J., Zhang, Z., Miller, W., and Lipman, D.J. (1997). Gapped BLAST and PSI-BLAST: a new generation of protein database search programs. Nucleic Acids Res. *25*, 3389–3402.

Aravind, L. (1999). An evolutionary classification of the metallo-beta-lactamase fold proteins. In Silico Biol. *1*, 69–91.

Aravind, L., and Koonin, E.V. (1998a). The HD domain defines a new superfamily of metal-dependent phosphohydrolases. Trends Biochem. Sci. *23*, 469–472.

Aravind, L., and Koonin, E.V. (1998b). A novel family of predicted phosphoesterases includes *Drosophila* prune protein and bacterial RecJ exonuclease. Trends Biochem. Sci. *23*, 17–19.

Beavo, J.A., and Brunton, L.L. (2002). Cyclic nucleotide research—still expanding after half a century. Nat. Rev. Mol. Cell Biol. *3*, 710–718.

Budd, G.T., Jayaraj, A., Grabowski, D., Adelstein, D., Bauer, L., Boyett, J., Bukowski, R., Murthy, S., and Weick, J. (1990). Phase I trial of dipyridamole with 5-fluorouracil and folinic acid. Cancer Res. *50*, 7206–7211.

Budd, G.T., Herzog, P., and Bukowski, R.M. (1994). Phase I/II trial of dipyridamole, 5-fluorouracil, leukovorin, and mitoxantrone in metastatic breast cancer. Invest. New Drugs *12*, 283–287.

Chang, C.L., Zhu, X.X., Thoraval, D.H., Ungar, D., Rawwas, J., Hora, N., Strahler, J.R., Hanash, S.M., and Radany, E. (1994). Nm23–H1 mutation in neuroblastoma. Nature *370*, 335–336.

Fan, Z., Beresford, P.J., Oh, D.Y., Zhang, D., and Lieberman, J. (2003). Tumor suppressor NM23–H1 is a granzyme A-activated DNase during CTL-mediated apoptosis, and the nucleosome assembly protein SET is its inhibitor. Cell *112*, 659–672.

Fisher, D.A., Smith, J.F., Pillar, J.S., St Denis, S.H., and Cheng, J.B. (1998). Isolation and characterization of PDE9A, a novel human cGMP-specific phosphodiesterase. J. Biol. Chem. *273*, 15559–15564.

Florenes, V.A., Aamdal, S., Myklebost, O., Maelandsmo, G.M., Bruland, O.S., and Fodstad, O. (1992). Levels of nm23 messenger RNA in metastatic malignant melanomas: inverse correlation to disease progression. Cancer Res. *52*, 6088–6091.

Forus, A., D'Angelo, A., Henriksen, J., Merla, G., Maelandsmo, G.M., Florenes, V.A., Olivieri, S., Bjerkehagen, B., Meza-Zepeda, L.A., del Vecchio Blanco, F., et al. (2001). Amplification and overexpression of PRUNE in human sarcomas and breast carcinomas-a possible mechanism for altering the nm23–H1 activity. Oncogene *20*, 6881–6890.

Freije, J.M., Blay, P., MacDonald, N.J., Manrow, R.E., and Steeg, P.S. (1997a). Site-directed mutation of Nm23–H1. Mutations lacking motility suppressive capacity upon transfection are deficient in histidine-dependent protein phosphotransferase pathways in vitro. J. Biol. Chem. *272*, 5525–5532.

Freije, J.M., Lawrence, J.A., Hollingshead, M.G., De la Rosa, A., Narayanan, V., Grever, M., Sausville, E.A., Paull, K., and Steeg, P.S. (1997b). Identification of compounds with preferential inhibitory activity against low-Nm23-expressing human breast carcinoma and melanoma cell lines. Nat. Med. *3*, 395–401.

Galperin, M.Y., Natale, D.A., Aravind, L., and Koonin, E.V. (1999). A specialized version of the HD hydrolase domain implicated in signal transduction. J. Mol. Microbiol. Biotechnol. *1*, 303–305.

Garzia, L., Andre, A., Amoresano, A., D'Angelo, A., Martusciello, R., Cirulli,

C., Tsurumi, T., Marino, G., and Zollo, M. (2003). Method to express and purify nm23–H2 protein from Baculovirus infected cells. Biotechniques *35*, 384–391.

Guex, N., and Peitsch, M.C. (1997). SWISS-MODEL and the Swiss-PdbViewer: an environment for comparative protein modeling. Electrophoresis *18*, 2714–2723.

Haaz, M.C., Fischel, J.L., Formento, P., Renee, N., Etienne, M.C., and Milano, G. (1996). Impact of different fluorouracil biochemical modulators on cellular dihydropyrimidine dehydrogenase. Cancer Chemother. Pharmacol. *38*, 52–58.

Hartsough, M.T., and Steeg, P.S. (1998). Nm23–H1: genetic alterations and expression patterns in tumor metastasis. Am. J. Hum. Genet. *63*, 6–10.

Hartsough, M.T., and Steeg, P.S. (2000). Nm23/nucleoside diphosphate kinase in human cancers. J. Bioenerg. Biomembr. *32*, 301–308.

Hartsough, M.T., Clare, S.E., Mair, M., Elkahloun, A.G., Sgroi, D., Osborne, C.K., Clark, G., and Steeg, P.S. (2001). Elevation of breast carcinoma Nm23–H1 metastasis suppressor gene expression and reduced motility by DNA methylation inhibition. Cancer Res. *61*, 2320–2327.

Hejna, M., Raderer, M., and Zielinski, C.C. (1999). Inhibition of metastases by anticoagulants. J. Natl. Cancer Inst. *91*, 22–36.

Howlett, A.R., Petersen, O.W., Steeg, P.S., and Bissell, M.J. (1994). A novel function for the nm23–H1 gene: overexpression in human breast carcinoma cells leads to the formation of basement membrane and growth arrest. J. Natl. Cancer Inst. *86*, 1838–1844.

Kantor, J.D., McCormick, B., Steeg, P.S., and Zetter, B.R. (1993). Inhibition of cell motility after nm23 transfection of human and murine tumor cells. Cancer Res. *53*, 1971–1973.

Leone, A., Flatow, U., VanHoutte, K., and Steeg, P.S. (1993a). Transfection of human nm23-H1 into the human MDA-MB-435 breast carcinoma cell line: effects on tumor metastatic potential, colonization and enzymatic activity. Oncogene *8*, 2325–2333.

Leone, A., Seeger, R.C., Hong, C.M., Hu, Y.Y., Arboleda, M.J., Brodeur, G.M., Stram, D., Slamon, D.J., and Steeg, P.S. (1993b). Evidence for nm23 RNA overexpression, DNA amplification and mutation in aggressive childhood neuroblastomas. Oncogene *8*, 855–865.

Lombardi, D., Lacombe, M.L., and Paggi, M.G. (2000). Nm23: unraveling its biological function in cell differentiation. J. Cell. Physiol. *182*, 144–149.

MacDonald, N.J., Freije, J.M., Stracke, M.L., Manrow, R.E., and Steeg, P.S. (1996). Site-directed mutagenesis of nm23–H1. Mutation of proline 96 or serine 120 abrogates its motility inhibitory activity upon transfection into human breast carcinoma cells. J. Biol. Chem. *271*, 25107–25116.

Mao, H., Liu, H., Fu, X., Fang, Z., Abrams, J., and Worsham, M.J. (2001). Loss of nm23 expression predicts distal metastases and poorer survival for breast cancer. Int. J. Oncol. *18*, 587–591.

Niitsu, N., Okabe-Kado, J., Okamoto, M., Takagi, T., Yoshida, T., Aoki, S., Hirano, M., and Honma, Y. (2001). Serum nm23–H1 protein as a prognostic factor in aggressive non-Hodgkin lymphoma. Blood *97*, 1202–1210.

Notredame, C., Higgins, D.G., and Heringa, J. (2000). T-Coffee: A novel method for fast and accurate multiple sequence alignment. J. Mol. Biol. *302*, 205–217.

Reymond, A., Volorio, S., Merla, G., Al-Maghtheh, M., Zuffardi, O., Bulfone, A., Ballabio, A., and Zollo, M. (1999). Evidence for interaction between human PRUNE and nm23–H1 NDPKinase. Oncogene *18*, 7244–7252.

Sleeman, J.P. (2000). The lymph node as a bridgehead in the metastatic dissemination of tumors. Recent Results Cancer Res. *157*, 55–81.

Steeg, P.S. (2003). Metastasis suppressors alter the signal transduction of cancer cells. Nat. Rev. Cancer *3*, 55–63.

Timmons, L., and Shearn, A. (1996). Germline transformation using a prune cDNA rescues prune/killer of prune lethality and the prune eye color phenotype in Drosophila. Genetics *144*, 1589–1600.

Tseng, Y.H., Vicent, D., Zhu, J., Niu, Y., Adeyinka, A., Moyers, J.S., Watson, P.H., and Kahn, C.R. (2001). Regulation of growth and tumorigenicity of breast cancer cells by the low molecular weight GTPase Rad and nm23. Cancer Res. *61*, 2071–2079.

Wagner, P.D., Steeg, P.S., and Vu, N.D. (1997). Two-component kinase-like activity of nm23 correlates with its motility-suppressing activity. Proc. Natl. Acad. Sci. USA *94*, 9000–9005.

Yamagata, A., Kakuta, Y., Masui, R., and Fukuyama, K. (2002). The crystal structure of exonuclease RecJ bound to Mn2+ ion suggests how its characteristic motifs are involved in exonuclease activity. Proc. Natl. Acad. Sci. USA *99*, 5908–5912.